

Frenkel Exciton-Polaritons in Organic Photonics

Boris Fainberg

Faculty of Sciences, Holon Institute of Technology, Holon, Israel

Tel Aviv University, School of Chemistry, Tel Aviv, Israel

*corresponding author, E-mail: fainberg@hit.ac.il

Abstract

We develop a mean-field electron-vibrational theory of Frenkel exciton polaritons in organic dye structures. The theory contains experimentally measured quantities that make it closely related to experiment, and provides a possibility of generalization to a nonlinear regime. Between other things, we explain the additional red shift of the H-aggregate absorption spectra (that are blue-shifted as a whole). We apply the theory to experiment on fraction of a millimeter propagation of Frenkel exciton polaritons in photoexcited organic nanofibers made of thiacyanine dye. A good agreement between theory and experiment is obtained.

1. Introduction

Recently organic dye nanofibers demonstrated long-range Frenkel exciton polariton (EP) propagation at room temperature [1, 2]. EPs are new quasi-particles formed when the coupling between excitons and photons in condensed matter is strong. They combine exciton and photon properties.

The long-range Frenkel EPs are formed in organic dye nanofibers at room temperatures owing to a considerably larger oscillator strength compared to inorganic semiconductors [1]. To realize such long-range propagation, the Frenkel EPs should be stable. Their stability is governed by splitting between two branches of the polariton dispersion, the correct calculation of which is of decisive importance. The latter necessitates the proper description of the Frenkel exciton line shape that is impossible without taking the electron-vibrational interaction into account (especially for H-aggregates, as it took place in experiment [1]). In other words, we need in an EP theory that takes electron-vibrational interaction into account in a simple way and provides a possibility of generalization to a nonlinear regime.

In this work we develop a mean-field electron-vibrational theory of Frenkel EPs in organic dye structures and apply it to experiment [1]. Our consideration is based on the model of the interaction of strong shaped laser pulse with organic molecules, Refs.[3, 4, 5], extended to the dipole-dipole intermolecular interactions in the condensed matter. These latter results in two options: one mother - two daughters. The first option correctly describes the behaviour of the first moment of molecular spectra in condensed matter, and specifically, the red shift, according

to the Clausius-Mossotti Lorentz-Lorentz (CMLL) mechanism [6]. The second option is related to the dramatic modification of molecular spectra in condensed matter due to aggregation of molecules into J- or H-aggregates. The theory contains experimentally measured quantities that make it closely related to experiment. Between other things, using the first option, we explain the additional red shift of the H-aggregate experimental absorption spectra [7] (that are blue-shifted as a whole, and the lineshape of which is described by the second option).

2. Derivation of equations for dipole-dipole intermolecular interactions in condensed matter

In this section we shall extend equations for vibrationally non-equilibrium populations of molecular electronic states of Refs. [3, 4, 5] to a condensed matter. In this picture we considered a molecule with two electronic states $n = 1$ (ground) and 2 (excited) in a solvent described by the Hamiltonian

$$H_0 = \sum_{n=1}^2 |n\rangle [E_n + W_n(\mathbf{Q})] \langle n| \quad (1)$$

where $E_2 > E_1$, E_n is the energy of state n , $W_n(\mathbf{Q})$ is the adiabatic Hamiltonian of reservoir R (the vibrational subsystems of a molecule and a solvent interacting with the two-level electron system under consideration in state n). The molecule is affected by electromagnetic field $\mathbf{E}(t)$

$$\mathbf{E}(t) = \frac{1}{2} \mathbf{e} \mathcal{E}(t) \exp(-i\omega t) + \text{c.c.} \quad (2)$$

the frequency of which is close to that of the transition $1 \rightarrow 2$. Here $\mathcal{E}(t)$ describes the change of the pulse amplitude in time, \mathbf{e} is unit polarization vector.

Since an absorption spectrum of a large molecule in condensed matter consists from overlapping vibronic transitions, we shall single out the contribution from the low frequency (LF) optically active (OA) vibrations $\{\omega_s\}$ to $W_n(\mathbf{Q})$: $W_n(\mathbf{Q}) = W_{nM} + W_{ns}$ where W_{ns} is the sum of the Hamiltonian governing the nuclear degrees of freedom of the solvent in the absence of the solute and LFOA intramolecular vibrations, and the part which describes interactions between the solute and the nuclear degrees of freedom of the solvent; W_{nM} is the Hamiltonian representing

the nuclear degrees of freedom of the high frequency (HF) OA vibrations of the solute molecule.

The influence of the vibrational subsystems of a molecule and a solvent on the electronic transition within the range of definite vibronic transition related to HFOA vibration ($\approx 1000 - 1500 \text{ cm}^{-1}$) can be described as a modulation of this transition by LFOA vibrations $\{\omega_s\}$ [8]. We suppose that $\hbar\omega_s \ll k_B T$. Thus $\{\omega_s\}$ is an almost classical system. In accordance with the Franck-Condon principle, an optical electronic transition takes place at a fixed nuclear configuration. Therefore, the quantity $u_{1s}(\mathbf{Q}) = W_{2s}(\mathbf{Q}) - W_{1s}(\mathbf{Q}) - \langle W_{2s}(\mathbf{Q}) - W_{1s}(\mathbf{Q}) \rangle_1$ representing electron-vibration coupling is the disturbance of nuclear motion under electronic transition where $\langle \rangle_n$ stands for the trace operation over the reservoir variables in the electronic state n . Electronic transition relaxation stimulated by LFOA vibrations is described by the correlation function $K(t) = \langle \alpha(0)\alpha(t) \rangle$ of the corresponding vibrational disturbance with characteristic attenuation time τ_s [9, 10, 11] where $\alpha \equiv -u_{1s}/\hbar$. The analytic solution of the problem under consideration has been obtained due to the presence of a small parameter. For broad vibronic spectra satisfying the "slow modulation" limit, we have $\sigma_{2s}\tau_s^2 \gg 1$ where $\sigma_{2s} = K(0)$ is the LFOA vibration contribution to a second central moment of an absorption spectrum, the half bandwidth of which is related to σ_{2s} as $\Delta\omega_{abs} = 2\sqrt{2}\sigma_{2s}\ln 2$. According to Refs. [10, 11], the following times are characteristic for the time evolution of the system under consideration: $\sigma_{2s}^{-1/2} < T' \ll \tau_s$, where $\sigma_{2s}^{-1/2}$ and $T' = (\tau_s/\sigma_{2s})^{1/3}$ are the times of reversible and irreversible dephasing of the electronic transition, respectively. The characteristic frequency range of changing the optical transition probability can be evaluated as the inverse T' , i.e. $(T')^{-1}$. Thus, one can consider T' as a time of the optical electronic transition. Therefore, the inequality $\tau_s \gg T'$ implies that the optical transition is instantaneous where relation $T'/\tau_s \ll 1$ plays the role of a small parameter. This made it possible to describe vibrationally non-equilibrium populations in electronic states 1 and 2 $\rho_{jj}(\alpha, t)$ ($j = 1, 2$) by balance equations for the intense pulse excitation (pulse duration $t_p > T'$) and solve the problem [12, 3, 4, 5]. For brevity, we consider here only one vibronic transition related to a HFOA vibration. Generalization to the case of a number of vibronic transitions will be made below.

The equation under discussion were written for the partial density matrix of the system $\rho_{jj}(\alpha, t)$ that described the system distribution in states 1 and 2 with a given value of α at time t . The complete density matrix averaged over the stochastic process which modulates the system energy levels, is obtained by integration of $\rho_{ij}(\alpha, t)$ over α , $\langle \rho \rangle_{ij}(t) = \int \rho_{ij}(\alpha, t) d\alpha$, where quantities $\langle \rho \rangle_{jj}(t)$ are the normalized populations of the corresponding electronic states: $\langle \rho \rangle_{jj}(t) \equiv n_j$, $n_1 + n_2 = 1$. Knowing $\rho_{jj}(\alpha, t)$, one can calculate the positive frequency component of the polarization $\mathbf{P}^{(+)}(t) = N\mathbf{D}_{12}\langle \rho \rangle_{21}(t)$, and the susceptibility $\chi(\Omega, t)$ [3] that enables us to obtain the dielectric

function ε due to relation $\varepsilon(\Omega, t) = 1 + 4\pi\chi(\Omega, t)$. Here N is the density of molecules, and \mathbf{D}_{12} is the electronic matrix element of the dipole moment operator. It is worthy to note that magnitude $\varepsilon(\Omega, t)$ does make sense, since it changes in time slowly with respect to dephasing. In other words, $\varepsilon(\Omega, t)$ changes in time slowly with respect to reciprocal characteristic frequency domain of changing $\varepsilon(\Omega)$.

Let us include now the dipole-dipole intermolecular interactions in the condensed matter that are described by Hamiltonian [13, 9] $H_{int} = \hbar \sum_{m \neq n} J_{mn} b_m^\dagger b_n$ where J_{mn} is the resonant exciton coupling. Let us discuss the contribution of Hamiltonian \hat{H}_{int} to the change of $\rho_{ij}(\alpha, t)$ in time. In other words, we shall generalize Eq.(11) of Ref.[3] to the dipole-dipole intermolecular interactions in the condensed matter. Using the Heisenberg equations of motion, one obtains that \hat{H}_{int} gives the following contribution to the change of the expectation value of excitonic operator b_k in time

$$\begin{aligned} \frac{d}{dt} \langle b_k \rangle &\sim \frac{i}{\hbar} \langle [\hat{H}_{int}, b_k] \rangle \equiv \frac{i}{\hbar} \text{Tr}([\hat{H}_{int}, b_k] \rho) \\ &= -i \sum_{n \neq k} J_{kn} \langle (\hat{n}_{k1} - \hat{n}_{k2}) b_n \rangle \end{aligned} \quad (3)$$

where $\hat{n}_{k1} = b_k b_k^\dagger$, and $\hat{n}_{k2} = b_k^\dagger b_k$ is the exciton population operator. Considering an assembly of identical molecules, one can write $\langle b_k \rangle = \rho_{21}(\alpha, t)$ [14] if averaging in Eq.(3) is carried out using density matrix $\rho(\alpha, t)$. Consider the expectation value $\langle (\hat{n}_{k1} - \hat{n}_{k2}) b_n \rangle = \text{Tr}[(\hat{n}_{k1} - \hat{n}_{k2}) b_n \rho(\alpha_k, \alpha_n, t)]$ for $n \neq k$ where α_m is the effective vibrational coordinate of a molecule m ($m = k, n$). Due to fast dephasing (see above), it makes sense to neglect all correlations among different molecules [9], and set $\langle (\hat{n}_{k1} - \hat{n}_{k2}) b_n \rangle = \langle \hat{n}_{k1} - \hat{n}_{k2} \rangle \langle b_n \rangle$ and correspondingly $\rho(\alpha_k, \alpha_n, t) \simeq \rho(\alpha_k, t) \rho(\alpha_n, t)$, i.e. density matrix $\rho(\alpha_k, \alpha_n, t)$ is factorized. Here from dimension consideration one expectation value should be calculated using density matrix $\rho(\alpha, t)$, and another one - using $\langle \rho \rangle(t) = \int \rho(\alpha, t) d\alpha$. Since we sum with respect to n , it would appear reasonable to integrate with respect to α_n . However, this issue is not so simple. The point is that in addition to intramolecular vibrations, there is a contribution of low-frequency intermolecular and solvent coordinates into effective coordinate α . Because of this, partitioning the vibrations into α_k and α_n groups is ambiguous, and the mean-field approximation gives two options

$$p \langle b \rangle \langle \hat{n}_1 - \hat{n}_2 \rangle = \left(\begin{array}{c} p \rho_{21}(\alpha, t) \Delta n \\ p \langle \rho_{21} \rangle(t) \Delta'(\alpha, t) \end{array} \right) \quad (4)$$

where $\Delta'(\alpha, t) = \rho_{11}(\alpha, t) - \rho_{22}(\alpha, t)$, $p \equiv -\sum_{n \neq k} J_{kn}$, $\Delta n \equiv n_1 - n_2$. Below we shall discuss which option better corresponds to a specific experimental situation. Consideration based on non-equilibrium Green functions (GF) shows that the terms $p \rho_{21}(\alpha, t)$ and $p \langle \rho_{21} \rangle(t)$ on the right-hand-side of Eq.(4) represent the self-energy, $i\Sigma_{21}(t)$, and the terms Δn and $\Delta'(\alpha, t)$ - the difference of the "lesser" GFs for equal time arguments, $\frac{i\hbar}{N} [G_{11}^<(t, t) -$

$G_{22}^<(t, t)$], that are the density matrix, i.e. $p\langle b \rangle \langle \hat{n}_1 - \hat{n}_2 \rangle = -\frac{\hbar}{N}\Sigma_{21}(t)[G_{11}^<(t, t) - G_{22}^<(t, t)]$, respectively. In other words, for the first line on the right-hand-side of Eq.(4), the self-energy depends on α and the "lesser" GFs $G_{11}^<(t, t) - G_{22}^<(t, t)$ do not. In contrast, for the second line on the right-hand-side of Eq.(4), the self-energy does not depend on α and the "lesser" GFs $G_{11}^<(\alpha; t, t) - G_{22}^<(\alpha; t, t)$ do depend. This yields $\partial\rho_{21}(\alpha, t)/\partial t \sim -\frac{i\hbar}{N}\Sigma_{21}(t)[G_{11}^<(t, t) - G_{22}^<(t, t)]$. Adding term $-\frac{i\hbar}{N}\Sigma_{21}(t)[G_{11}^<(t, t) - G_{22}^<(t, t)]$ to the right-hand side of Eq.(9) of Ref.[3] for the non-diagonal density matrix $\tilde{\rho}_{21}(\alpha, t)$

$$\begin{aligned} & \frac{\partial}{\partial t}\tilde{\rho}_{21}(\alpha, t) + i(\omega_{21} - \omega - \alpha)\tilde{\rho}_{21}(\alpha, t) \\ & \approx \frac{i}{2\hbar}\mathbf{D}_{21} \cdot \mathbf{E}(t)\Delta'(\alpha, t) - i\frac{\hbar}{N}\tilde{\Sigma}_{21}(t)[G_{11}^<(t, t) \\ & \quad - G_{22}^<(t, t)] \end{aligned} \quad (5)$$

where ω_{21} is the frequency of Franck-Condon transition $1 \rightarrow 2$, $\tilde{\rho}_{21} = \rho_{21} \exp(i\omega t)$, $\tilde{\Sigma}_{21} = \Sigma_{21} \exp(i\omega t)$, and using the procedure described there, we get the extensions of Eq.(11) of Ref.[3] to the dipole-dipole intermolecular interactions in the condensed matter.

Consider first the case of self-energy depending on effective vibrational coordinate α (the first line on the right-hand-side of Eq.(4)) when the main contribution to α is due to low-frequency intermolecular vibrations and solvent coordinates. Then we obtain Eq.(1) of Ref.[15] (see Appendix 1). In that case, as one can see from Eq.(27) of Appendix 1, the self-energy $i\Sigma_{21}(t) = p\rho_{21}(\alpha, t)$ results in the frequency shift of spectra $-p\Delta n$ without changing the line shapes. One can show that this approach correctly describes the change of the first moment of optical spectra in the condensed matter. Calculations of p for isotropic medium give $p = \frac{4\pi}{3\hbar}|D_{12}|^2N > 0$ [9, 15] that corresponds to a red shift, according to the Clausius-Mossotti Lorentz-Lorentz (CMLL) mechanism [6].

Let us consider the particular case of fast vibrational relaxation. Physically it means that the equilibrium distributions into the electronic states have had time to be set during changing the pulse parameters. In that case one gets the equations for the populations of electronic states $n_{1,2}$ (see Appendix 1)

$$\begin{aligned} \frac{dn_j}{dt} &= (-1)^j\sigma_a(\omega_{21})\tilde{J}(t)\text{Re}[n_1\bar{W}_a(\omega + p\Delta n) - \\ &\quad - n_2\bar{W}_f(\omega + p\Delta n)] - (-1)^j\frac{n_2}{T_1} \end{aligned} \quad (6)$$

where $n_1 + n_2 = 1$, σ_a is the cross section at the maximum of the absorption band, $\tilde{J}(t)$ is the power density of exciting radiation, $\bar{W}_a(\omega) = W_a(\omega)/F_{a,\text{max}}$, $F_{a,\text{max}}$ is the maximum value of the absorption line (see below), and we added term $"(-1)^j n_2/T_1"$ taking the lifetime T_1 of the excited state into account. Here $-iW_{a(f)}(\omega)$ is the line-shape function of a monomer molecule for the absorption (fluorescence) for fast vibronic relaxation. In the case

under consideration, it is related to the line-shape function, $\int d\alpha\Delta'(\alpha, t)\zeta(\omega - \omega_{21} + \alpha)/\pi$, by formula

$$\begin{aligned} & \int_{-\infty}^{\infty} d\alpha\Delta'(\alpha, t)\zeta(\omega - \omega_{21} + \alpha)/\pi \\ & = -i[n_1(t)W_a(\omega) - n_2(t)W_f(\omega)] \end{aligned} \quad (7)$$

where $\zeta(\omega - \omega_{21} + \alpha) = \frac{P}{\omega - \omega_{21} + \alpha} - i\pi\delta(\omega - \omega_{21} + \alpha)$, P is the symbol of the principal value.

The imaginary part of $"-iW_{a(f)}(\omega)"$ with sign minus, $-\text{Im}[-iW_{a(f)}(\omega)] = \text{Re}W_{a(f)}(\omega) \equiv F_{a(f)}(\omega)$, describes the absorption (fluorescence) line-shapes of a monomer molecule, and the real part, $\text{Re}[-iW_{a(f)}(\omega)] = \text{Im}W_{a(f)}(\omega)$, describes the corresponding refraction spectra. For the "slow modulation" limit considered in the beginning of this section, quantities $W_{a(f)}(\omega)$ and $F_{a(f)}(\omega)$ are given by Eqs. (30) and (31), respectively, of Appendix 1.

2.1. Population difference ("lesser" GFs) depending on effective vibrational coordinate α

Consider now the case when the population difference depends on effective vibrational coordinate α (the second line on the right-hand-side of Eq.(4); the main contribution to α is due to intramolecular vibrations). Then using Eq.(24) of Appendix 1 and Eq.(5), we arrive to equation

$$\begin{aligned} \frac{\partial\rho_{jj}(\alpha, t)}{\partial t} &= L_{jj}\rho_{jj}(\alpha, t) + \frac{(-1)^j\pi}{2}\Delta'(\alpha, t) \\ &\quad \times \delta(\omega_{21} - \omega - \alpha)|\Omega_{\text{eff}}(t)|^2 \end{aligned} \quad (8)$$

where $\Omega_{\text{eff}}(t) = \Omega_R(t) + 2p\langle\rho_{21}\rangle(t) = \Omega_R(t) + 2\Sigma_{21}(t)$ is the effective Rabi frequency that can be written as

$$\Omega_{\text{eff}}(t) = \frac{\Omega_R(t)}{1 + p\int d\alpha\Delta'(\alpha, t)\zeta(\omega - \omega_{21} + \alpha)}, \quad (9)$$

Here $\Omega_R(t) = (\mathbf{D}_{12} \cdot \mathbf{e})\mathcal{E}(t)/\hbar$ is the Rabi frequency, operator L_{jj} describes the diffusion with respect to the coordinate α in the corresponding effective parabolic potential, Eq.(25) of Appendix 1.

One can see that in contrast to the self-energy depending on effective vibrational coordinate α (see above), here the self-energy $\Sigma_{21}(t) = -ip\langle\rho_{21}\rangle(t)$ (the second line on the right-hand-side of Eq.(4)) results in the change of both the frequency shift of spectra and their line-shapes. In that case considering the dense collection of molecules under the action of one more (weak) field $\tilde{\mathbf{E}}(t) = \frac{1}{2}\mathbf{e}\tilde{\mathcal{E}}(t)\exp(-i\Omega t) + \text{c.c.}$, one can calculate the susceptibility $\chi(\Omega, t) = P^+(\Omega, t)/(\tilde{\mathcal{E}}(t)/2)$ related to the positive frequency component of the polarization $\mathbf{P}^+ = ND_{12}\langle\rho_{21}\rangle(t)$, and the dielectric function $\varepsilon(\Omega) = \varepsilon_0(1 + 4\pi\chi(\Omega))$ [16] that in our case is given by

$$\varepsilon(\Omega, t) = \varepsilon_0\left[1 - \frac{q\int d\alpha\Delta'(\alpha, t)\zeta(\Omega - \omega_{21} + \alpha)}{1 + p\int d\alpha\Delta'(\alpha, t)\zeta(\Omega - \omega_{21} + \alpha)}\right] \quad (10)$$

Here $\varepsilon_0 = n_0^2$, n_0 is the background refractive index of the medium, $q \equiv 4\pi\eta \frac{N|\mathbf{D}_{12}|^2}{\hbar}$, $\eta = 1/3$ for randomly oriented molecules, and $\eta = 1$ for the molecules of the same orientation.

2.1.1. Line-shape in the fast vibrational relaxation limit

Below we shall see that the approximation based on the self-energy integrated on the effective vibrational coordinate (the second line on the right-hand-side of Eq.(4)) correctly describe the exciton spectra. In that case the fast vibrational relaxation limit should be based on the equilibrium state of the collective system (molecules coupled by the dipole-dipole interaction). However, the exciton wave function in the ground state is the product of the wave functions of monomers [13] (no intermolecular interactions). Because of this, for the absorption of weak radiation, one should put $j = 1$ and $\Delta'(\alpha, t) = \Delta'^{(0)}(\alpha)$ in Eqs. (8) and (9) where $\Delta'^{(0)}(\alpha) = \rho_{11}^{(0)}(\alpha) = (2\pi\sigma_{2s})^{-1/2} \exp[-\alpha^2/(2\sigma_{2s}^2)]$ is the equilibrium value of $\Delta'(\alpha, t)$ corresponding to the equilibrium value for a monomer in the ground state, and we retained only terms that are proportional to $|\Omega_R(t)|^2$ on the right-hand side of Eq.(8). The next procedure is similar to that used for obtaining Eq.(6) (see Appendix 1). Integrating Eq.(8) using Green function [12], we obtain an integral equation. Then integrating both sides of the obtained integral equation with respect to α , and bearing in mind Eq.(7), we get

$$\frac{dn_1}{dt} = -\sigma_a(\omega_{21})\tilde{J}(t)\text{Re}\frac{\bar{W}_a(\omega)}{1 - ip\pi W_a(\omega)} + \frac{n_2}{T_1} \quad (11)$$

where the term $\text{Re}\{\bar{W}_a(\omega)/[1 - ip\pi W_a(\omega)]\}$ describes the absorption spectrum of molecules susceptible to the dipole-dipole intermolecular interactions expressed through their monomer spectra W_a . The calculation results of the absorption spectra of J-aggregates according to the expression $\text{Re}\{W_a(\omega)/[1 - ip\pi W_a(\omega)]\}$ are given in Appendix 2.

Touching on how Eq.(11) can be extended to stronger radiation, one should recognize two limit cases. In the first case an optical transitions occur near zero quasi-momentum $\mathbf{k} \approx 0$. After the light absorption a quasi-equilibrium is established. However, the luminescence should be resonant to the absorption line due to the quasi-momentum conservation [13]. This case is realized for J-aggregates [17]. The second case is characterized by a strong electron-vibrational interaction when the relaxation to the equilibrium vibrational configuration in the excited state occurs before the excitation transfers to the neighboring molecule [18]. It seems such a case is realized for the H-aggregates of thiacyanine (TC) dye molecules where a large Stokes shift between absorption and photoluminescence spectra of the TC aggregates was observed in the aqueous solution [19, 20]. Since the description of the H-aggregate spectra necessitates including also the HFOA vibrations and the mechanism described by Eq.(6) (see Section 3), the extension to stronger radiation for H-aggregates will be carried out elsewhere.

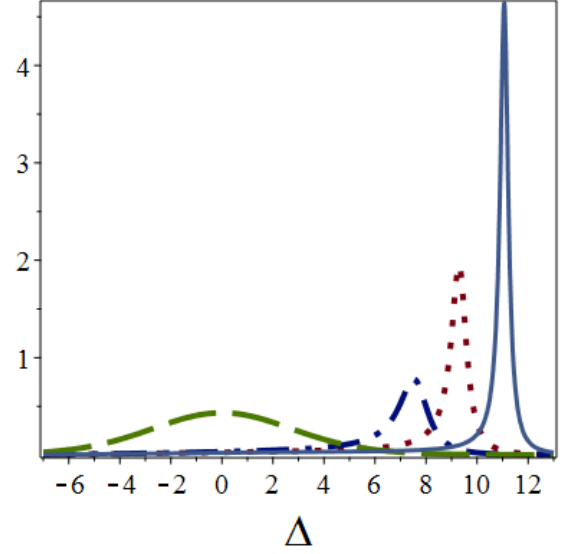


Figure 1: Nonlinear absorption spectra (in terms of τ_s/π) of the J-aggregate for $\Delta n = 1$ (solid line), $\Delta n = 0.8$ (dotted line), $\Delta n = 0.6$ (dash dotted line), and the corresponding monomer absorption spectrum (dashed line) for $\sqrt{\sigma_{2s}\tau_s} = 3.16$ and $p\tau_s = 10$. Dimensionless parameter is $\Delta = \tau_s(\omega_{21} - \omega)$, $\tau_s/(2T_1) \ll 1$.

For the first case one can put $\Delta'(\alpha, t) = \Delta n (2\pi\sigma_{2s})^{-1/2} \exp[-\alpha^2/(2\sigma_{2s}^2)]$ in Eqs. (8) and (9), and we obtain the extension of Eq.(11) to stronger radiation

$$\frac{dn_1}{dt} = -\sigma_a(\omega_{21})\tilde{J}(t)\text{Re}\frac{\Delta n \bar{W}_a(\omega)}{1 - ip\pi \Delta n W_a(\omega)} + \frac{n_2}{T_1} \quad (12)$$

In Eq.(12) the probability of the light induced transitions may be of the same order of magnitude as T_1^{-1} , however, the first should be smaller than the reciprocal dephasing time.

The term $\text{Re}\frac{\Delta n \bar{W}_a(\omega)}{1 - ip\pi \Delta n W_a(\omega)}$ on the right-hand-side of Eq.(12) describes a nonlinear absorption. In particular case of weak radiation when $\Delta n = 1$, this term recovers the coherent exciton scattering (CES) approximation [21, 7, 22]. The latter is well suited to describing the absorption spectrum lineshape for J-aggregates using their monomer spectra and the intermolecular interaction strength that is a fitting parameter. As to the absorption spectra of H-aggregates, the CES approximation describes correctly only their lineshapes. The positions of the H-aggregate spectra calculated in the CES approximation should be corrected [7]. This issue will be considered in more details in Section 3, since we apply our theory to the EPs in H-aggregates of TC dye molecules below.

Fig.1 shows the calculation results of the nonlinear absorption spectra of J-aggregates according to the expression $\text{Re}\{\Delta n W_a(\omega)/[1 - ip\pi \Delta n W_a(\omega)]\}$ on the right-hand-side

of Eq.(12) for different values of the population difference Δn . The vibrationally equilibrium monomer absorption spectrum $W_a(\omega)$ was calculated using Eq.(36) of Appendix 2. The spectra of Fig.1 demonstrate the saturation effect accompanied by the blue shift of the spectra when the population difference Δn diminishes. Such a frequency shift arises also in the many-body theory of 1D Frenkel excitons [23] that does not consider the vibrations. In contrast, our theory does take the vibrations into account that enables us to correctly describe the lineshape of J-aggregates.

3. Proper description of the lineshape and the frequency shift of absorption spectra of H-aggregates

Applying expression $\text{Re}\{W_a(\omega)/[1 - ip\pi W_a(\omega)]\}$ (see Section 2.1.1) to the description of the absorption of H-aggregates, one should take into account also HFOA intramolecular vibrations, in addition to the LFOA vibrations $\{\omega_s\}$ under consideration in our paper. The intramolecular relaxation related to the OAHF vibrations takes place in a time shorter than intermolecular relaxation of the low frequency system $\{\omega_s\}$ [4, 24, 5]. Therefore, we can consider the density matrix averaged with respect to the intramolecular OAHF vibrations: $\rho_{ns}(t) = \text{Tr}_M \rho_{nn}(t)$ where the total density matrix $\rho_{nn}(t)$ is factorized, $\rho_{nn}(t) = \rho_{nM} \rho_{ns}(t)$, and $\rho_{nM} = \exp(-\beta W_{nM})/\text{Tr}_M \exp(-\beta W_{nM})$ is the equilibrium density matrix of the intramolecular OAHF vibrations. Here Tr_M denotes the operation of taking a trace over the variables of the intramolecular OAHF vibrations, $\beta = 1/(k_B T)$. Using density matrix ρ_{ns} , one can obtain an equation akin to Eq.(11) where the monomer spectrum is given by

$$W_a(\omega) = \frac{\tau_s}{\pi} \exp(-S_0) \sum_{k=0}^{\infty} \frac{S_0^k}{k!} \frac{\Phi(1, 1 + x_{ak}; \sigma_{2s} \tau_s^2)}{x_{ak}} \quad (13)$$

where $x_{ak} = \tau_s/(2T_1) + \sigma_{2s} \tau_s^2 + i\tau_s(\omega_{21} - \omega + k\omega_0)$. Eq.(13) is derived in Appendix 3 for the model of one normal high frequency intramolecular oscillator of frequency ω_0 whose equilibrium position is shifted under electronic transition (S_0 is the dimensionless parameter of the shift). Here $\Phi(1, 1 + x_a; \sigma_{2s} \tau_s^2)$ is a confluent hypergeometric function [25] the parameters of which are defined in Appendix 2.

As we mentioned above, expression $\text{Re}\{W_a(\omega)/[1 - ip\pi W_a(\omega)]\}$ corresponds to the CES approximation that describes well the shape of the absorption spectra of H-aggregates. However, the spectra calculated in the CES approximation are blue shifted with respect to experimental ones [7]. To resolve the problem, the authors of Ref.[7] empirically introduced additional red shift that can be substantiated in our more general theory. Indeed, let us write down Eq.(5) when both the self-energy ($\tilde{\rho}_{21}$) and the population difference depend on the effective vibrational coordinate

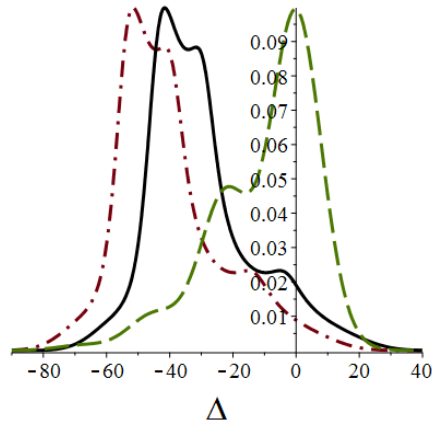


Figure 2: Absorption spectra (in terms of τ_s/π) of the H-aggregate (solid line), the corresponding monomer (dash line) and the H-aggregate without the contribution of the CMLL mechanism (dash dot line) for $p_1 = 500 \text{ cm}^{-1}$ and $p_2 = -1500 \text{ cm}^{-1}$. Dimensionless parameter is $\Delta = \tau_s(\omega_{21} - \omega)$.

$$\begin{aligned} & \frac{\partial}{\partial t} \tilde{\rho}_{21}(\alpha, t) + i(\omega_{21} - \omega - p_1 - \alpha) \tilde{\rho}_{21}(\alpha, t) \\ &= i \left[\frac{\mathbf{D}_{21} \cdot \mathbf{E}(t)}{2\hbar} + p_2 \int d\alpha \tilde{\rho}_{21}(\alpha, t) \right] \rho_{11}^{(0)}(\alpha) \quad (14) \end{aligned}$$

Using the procedure described in Ref.[3], we get an equation similar to Eq. (8) (together with Eq.(9)) with the only difference that ω_{21} should be replaced by $\omega_{21} - p_1$, and p - by p_2

$$\begin{aligned} \frac{\partial \rho_{11}(\alpha, t)}{\partial t} &= \frac{-\frac{\pi}{2} \rho_{11}^{(0)}(\alpha) |\Omega_R(t)|^2 \delta(\omega_{21} - \omega - p_1 - \alpha)}{\left| 1 + p_2 \int d\alpha \rho_{11}^{(0)}(\alpha) \zeta(\omega + p_1 - \omega_{21} + \alpha) \right|^2} \\ &+ L_{11} \rho_{11}(\alpha, t) \quad (15) \end{aligned}$$

Then similar to Eq.(11), we obtain

$$\frac{dn_1}{dt} = -\sigma_a(\omega_{21}) \tilde{J}(t) \text{Re} \frac{\bar{W}_a(\omega + p_1)}{1 - ip_2 \pi W_a(\omega + p_1)} + \frac{n_2}{T_1} \quad (16)$$

where the term $\text{Re}\{\bar{W}_a(\omega + p_1)/[1 - ip_2 \pi W_a(\omega + p_1)]\}$ describes the absorption spectrum of molecules susceptible to the dipole-dipole intermolecular interactions expressed through their monomer spectra $W_a(\omega + p_1)$, Eq.(13). Fig.2 shows the calculation results of the absorption spectrum of an H-aggregate according to the expression $\text{Re}\{W_a(\omega + p_1)/[1 - ip_2 \pi W_a(\omega + p_1)]\}$ on the right-hand side of Eq.(16) and Eq.(13) (solid line), and its comparison with the monomer spectrum $\text{Re}W_a(\omega)$ (dash line) and the spectrum of H-aggregate, $\text{Re}\{W_a(\omega)/[1 - ip_2 \pi W_a(\omega)]\}$, calculated without the contribution of the CMLL mechanism (dash dot line). The values of parameters are found by fitting the experimental spectrum of the linear absorption of

LD690 in methanol [5]: $\tau_s = 10^{-13} s$, $k_B T = 210 \text{ cm}^{-1}$, $\hbar \omega_{st}/(2k_B T) = 1.99$, $S_0 = 0.454$, $\omega_0 = 1130 \text{ cm}^{-1}$, $\sigma_{2s} = \omega_{st} k_B T / \hbar$. The spectra presented in Fig.2 manifest that though the shape of the H-aggregate spectrum is fully described by the self-energy not depending on the effective vibrational coordinate, its position (including the additional red shift of the experimental spectra of H-aggregates [7]) may be correctly described only taking the CMLL mechanism into account. In other words, our more general theory enables us to describe both the shape and the position of the experimental spectra of H-aggregates due to the self-energy and the population difference ("lesser" GFs) both depending on the effective vibrational coordinate that leads to their frequency dependence. This can be understood as follows. The frequency dependent "lesser" GFs corresponding to the CES approximation describe well the spectral shapes of H-aggregates. The latters can interact with each other by the dipole-dipole interaction leading to the CMLL red shift that is described by the frequency dependent self-energy.

In the case under consideration Eq.(10) for the dielectric function becomes

$$\varepsilon(\omega) = \varepsilon_0 \left[1 + \frac{i q \pi W_a(\omega + p_1)}{1 - i \pi p_2 W_a(\omega + p_1)} \right] \quad (17)$$

where we put $\int_{-\infty}^{\infty} d\alpha \Delta'^{(0)}(\alpha) \zeta(\omega - \omega_{21} + p_1 + \alpha) = -i\pi W_a(\omega + p_1)$ for the vibrational equilibrium in the ground state.

4. Application to the exciton-polariton experiment

The theory developed in Section 3 properly describes both the lineshape and the frequency shift of the absorption spectra of H-aggregates. Therefore, it can be applied to the experiment on fraction of a millimeter propagation of EPs in photoexcited fiber-shaped H-aggregates of TC dye at room temperature [1].

The transverse eigenmodes of the medium are obtained from the dispersion equation [16]

$$c^2 k^2(\omega) = \omega^2 \varepsilon(\omega) \quad (18)$$

where dielectric function $\varepsilon(\omega)$ is given by Eq.(17) and depends on the monomer spectra W_a .

Fig. 3 shows the experimental absorption lineshape of TC monomer solution prepared by dissolving TC dye in methanol [19] (top), and its theoretical description by $\text{Re}W_a$, Eq.(13), (bottom). Good agreement is observed with the values of parameters $\omega_{21} = 23810 \text{ cm}^{-1}$, $1/\tau_s = 75 \text{ cm}^{-1}$, $\omega_0 \tau_s = 20$, $S_0 = 0.454$, $\sigma_{2s} \tau_s^2 = 80$ obtained by comparison between experimental and theoretical curves.

The monomer spectrum found, W_a , enables us to calculate the aggregate absorption spectrum according to the formula $\text{Re}\{W_a(\omega + p_1)/[1 - i p_2 \pi W_a(\omega + p_1)]\}$ (see Eqs.(16) and (17) shown in Fig.4. Again good agreement between theoretical and experimental spectra is observed with the values of parameters $p_1 \tau_s = 4$, $p_2 \tau_s = -7$ obtained by comparison between experimental and theoretical curves.

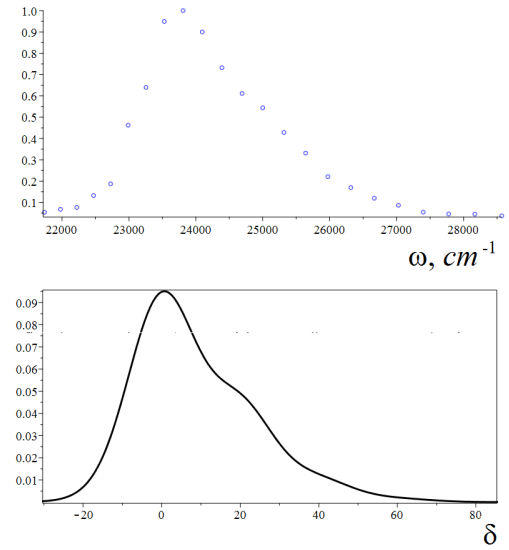


Figure 3: Experimental absorption lineshape of TC monomer solution prepared by dissolving TC dye in methanol [19] (top), and its theoretical description (in terms of τ_s/π) by $\text{Re}W_a$, Eq.(13), (bottom). Dimensionless parameter is $\delta = -\Delta = \tau_s(\omega - \omega_{21})$.

We did not make additional fitting since experimental absorption spectra of TC aggregates and monomers were measured in different solvents [19] (see caption to Fig.4).

4.1. Polariton dispersion

Let us analyze Eq.(18) where the dielectric function is determined by Eq.(17) and depends on the aggregate spectrum, $W_a(\omega + p_1)/[1 - i p_2 \pi W_a(\omega + p_1)]$. The parameters of the aggregate spectrum were found above. In order to satisfy Eq.(18), the wave number k should be complex $k = k' + i k''$. Then using Eq.(18), we get for the real and imaginary part of k

$$k' \frac{c}{n_0} = \omega \text{Re} \sqrt{1 + i \pi q \frac{W_a(\omega + p_1)}{1 - i \pi p_2 W_a(\omega + p_1)}} \quad (19)$$

and

$$k'' \frac{c}{n_0} = \omega \text{Im} \sqrt{1 + i \pi q \frac{W_a(\omega + p_1)}{1 - i \pi p_2 W_a(\omega + p_1)}}, \quad (20)$$

respectively. Fig.5 shows the Frenkel EP dispersion calculated using Eqs.(19) and (20).

To give physical insight into the Frenkel EP dispersion, we shall calculate also the dispersion outside the resonance when $k'' \approx 0$. In that case Eq.(18) leads to the undamped polariton modes

$$k' \frac{c}{n_0} \approx \omega \sqrt{1 - \pi q \text{Im} \frac{W_a(\omega + p_1)}{1 - i \pi p_2 W_a(\omega + p_1)}} \quad (21)$$

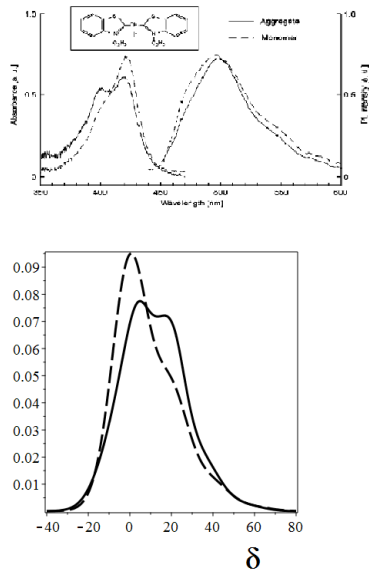


Figure 4: Experimental absorption and photoluminescence spectra of TC aggregates and monomers [19] (top), and theoretical description of aggregate absorption (in terms of τ_s/π) (bottom). In the top solid curve represents spectra of the aqueous solution containing TC aggregates; dashed curve, spectra of a monomer solution prepared by dissolving TC dye in methanol. In the bottom solid curve represents the spectrum of an aggregate; dashed curve - spectrum of a monomer. Dimensionless parameter $\delta = -\Delta = \tau_s(\omega - \omega_{21})$ increases when the wavelength decreases.

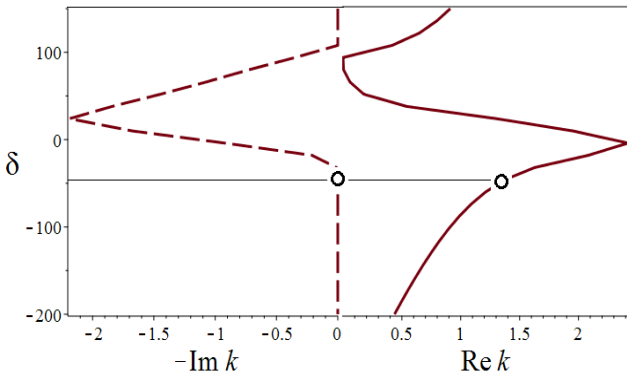


Figure 5: Frenkel EP dispersion for real (solid line) and imaginary (dashed line) part of the wave number k calculated with Eqs.(19) and (20), respectively, when $q\tau_s = 84$. Other parameters are identical to those of the bottom of Fig.3. k is in units of $c/(\omega_{21}n_0)$. Dimensionless parameter is $\delta = \tau_s(\omega - \omega_{21})$. Circles show the position of the fluorescence spectrum of a nanofiber.

Taking spectrum $W_a(\omega)$ to be centered on $\omega = \omega_a$ and to have a finite width Γ , it is clear from the dispersion relation [22] that $W_a(\omega) \sim (i/\pi)/(\omega - \omega_a)$ for $|\omega - \omega_a| \gg \Gamma$, and we get

$$k' \frac{c}{n_0} \approx \omega \sqrt{\frac{\omega - (\omega_a - p_1 - p_2) - q}{\omega - (\omega_a - p_1 - p_2)}} \quad (22)$$

Eq.(22) leads to two branches of the polariton dispersion shown in Fig.5, namely, the lower branch for $\omega < \omega_a - p_1 - p_2$, and the upper branch for $\omega > \omega_a - p_1 - p_2$. For $\omega \rightarrow \omega_a - p_1 - p_2$ the wavenumber diverges, $k' \rightarrow \infty$. No solution of Eq.(22) exists for frequencies between $\omega_a - p_1 - p_2$ and $(\omega_a - p_1 - p_2) + q$. In other words, there is a forbidden gap between $\omega_a - p_1 - p_2$ and $(\omega_a - p_1 - p_2) + q$ separating the lower and upper polariton branch. However, in the gap range more precise formulas, Eqs.(19) and (20), should be used, and the polariton dispersion shows the leaky part in the splitting range between two branches, Fig.5.

From Eq.(22) we get for low frequencies, $\omega \ll \omega_a - p_1 - p_2$, a photon-like dispersion

$$\omega \simeq \frac{ck'}{n_0 \sqrt{1 + q/(\omega_a - p_1 - p_2)}} \quad (23)$$

with a light velocity smaller than c/n_0 .

From the above discussion, it is evident that parameter $q = \frac{4\pi}{\hbar} \eta N |\mathbf{D}_{12}|^2$ defines the separation between the lower and upper polariton branch. For the molecules of the same orientation ($\eta = 1$) that corresponds to experiment [1], and $D_{12} \sim 10^{-17} CGSE$, $N = 10^{21} \text{ cm}^{-3}$, one obtains the evaluation $q \simeq 6322 \text{ cm}^{-1}$. This value agrees with the measurements of Ref.[1]. The position of the fluorescence spectrum of a nanofiber that is in the range of $\sim 2.5 \text{ eV}$ is shown as circles in Fig.5. One can see that it is located in the range where $\text{Im}k \approx 0$, and it is out of the splitting range under discussion. That is why the fluorescence was amplified well in experiment [1].

Fig.6 shows the real part of the group refraction index $n_g(\omega) = n(\omega) + \omega dn(\omega)/d\omega$ as a function of frequency where $n(\omega) = (c/\omega)k(\omega)$ is the phase refraction index. The curve of Fig.6 agrees with the experimental curve of Fig.2a of Ref.[1]. Both curves give the same value $\text{Ren}_g \approx 7$ at the position of the fluorescence spectrum of a nanofiber ($\sim 2.5 \text{ eV}$).

5. Conclusion

In this work we have developed a mean-field electron-vibrational theory of Frenkel EPs in organic dye structures. Our consideration is based on the model of the interaction of strong shaped laser pulse with organic molecules, Refs.[3, 4, 5], extended to the dipole-dipole intermolecular interactions in the condensed matter. We show that such a generalization can describe both a red shift of the resonance frequency of isolated molecules, according to the CMLL mechanism [6], and the wide variations of their spectra related to the aggregation of molecules into J- or H-aggregates. In particular case of weak radiation we recover

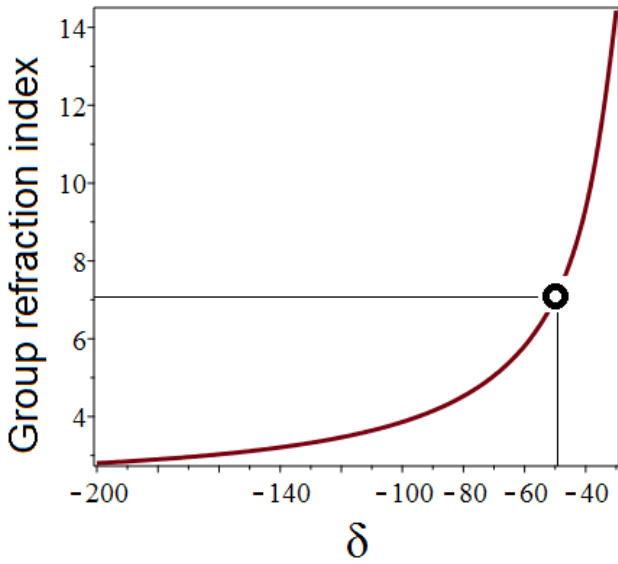


Figure 6: Real part of the group refraction index n_g for $n_0 = 1.5$. Other parameters are identical to those of Figs. 3 and 5. Circle shows the position of the fluorescence spectrum of a nanofiber. Parameter $\delta = \tau_s(\omega - \omega_{21})$.

the CES approximation [21, 7, 22]. We show that the experimental absorption spectra of H-aggregates may be correctly described only if one takes both mechanisms into account. Our theory contains experimentally measured quantities that makes it closely related to experiment, and provides a possibility of generalization to a nonlinear regime.

We have applied the theory to experiment on fraction of a millimeter propagation of Frenkel EPs in photoexcited organic nanofibers made of thiacyanine dye [1]. A good agreement between theory and experiment is obtained. The theory can be also applied to Frenkel EPs in organic microcavities [26] and to plexcitonics [27].

Acknowledgement

I thank G. Rosenman and B. Apter who attracted my attention to Ref. [1].

6. Appendix 1

In the presence of the dipole-dipole intermolecular interactions in the condensed matter Eq.(6) of Ref. [3] describing vibrationally non-equilibrium populations in electronic states $j = 1, 2$ for the exponential correlation function $K(t)/K(0) \equiv S(t) = \exp(-|t|/\tau_s)$ can be written as

$$\frac{\partial}{\partial t} \rho_{jj}(\alpha, t) = \frac{-i}{\hbar} [H_0(\alpha) + H_{int} - \mathbf{D} \cdot \mathbf{E}(t), \rho(\alpha, t)]_{jj} + L_{jj} \rho_{jj}(\alpha, t) \quad (24)$$

where $j = 1, 2$, and we added the term H_{int} into the Hamiltonian; the operator L_{jj} is determined by the equation:

$$L_{jj} = \tau_s^{-1} [1 + (\alpha - \delta_{j2}\omega_{st}) \frac{\partial}{\partial(\alpha - \delta_{j2}\omega_{st})} + \frac{\partial^2}{\partial(\alpha - \delta_{j2}\omega_{st})^2}], \quad (25)$$

describes the diffusion with respect to the coordinate α in the corresponding effective parabolic potential $U_j(\alpha)$, δ_{ij} is the Kronecker delta, $\omega_{st} = \beta\hbar\sigma_{2s}$ is the Stokes shift of the equilibrium absorption and luminescence spectra, $\beta = 1/k_B T$. In the absence of the dipole-dipole intermolecular interactions in the condensed matter, H_{int} , Eq.(24) is reduced to Eq.(11) of Ref.[3].

Consider first the case of self-energy depending on effective vibrational coordinate α (the first line on the right-hand-side of Eq.(4)) when the main contribution to α is due to low-frequency intermolecular vibrations and solvent coordinates. Then Eq.(5) becomes

$$\frac{\partial}{\partial t} \tilde{\rho}_{21}(\alpha, t) + i(\omega_{21} - \omega - p\Delta n - \alpha) \tilde{\rho}_{21}(\alpha, t) \approx \frac{i}{2\hbar} \mathbf{D}_{21} \cdot \mathbf{E}(t) \Delta'(\alpha, t) \quad (26)$$

Solving Eq.(26) for $\tilde{\rho}_{21}(\alpha, t)$ and substituting for the corresponding expression in Eq.(24), we we arrive to equation

$$\frac{\partial \rho_{jj}(\alpha, t)}{\partial t} = L_{jj} \rho_{jj}(\alpha, t) + \frac{(-1)^j \pi}{2} \Delta'(\alpha, t) |\Omega_R(t)|^2 \times \times \delta[\omega_{21} - p\Delta n - \omega - \alpha] \quad (27)$$

that was obtained in Ref.[15]. Here ω_{21} is the frequency of Franck-Condon transition $1 \rightarrow 2$, $\Omega_R(t) = (\mathbf{D}_{12} \cdot \mathbf{e}) \mathcal{E}(t)/\hbar$ is the Rabi frequency, \mathbf{D}_{12} is the electronic matrix element of the dipole moment operator. Integration of Eq.(27) is achieved by the Green's function [12]. Then integrating both sides of the obtained integral equation with respect to α , we get

$$\frac{dn_j}{dt} = (-1)^j \frac{\pi}{2} |\Omega_R(t)|^2 \Delta'(\omega_{21} - p\Delta n - \omega, t) \quad (28)$$

Let us consider the particular case of fast vibrational relaxation when one can put the normalized correlation function $S(t - t') \equiv K(t - t')/K(0)$ equal to zero. Physically it means that the equilibrium distributions into the electronic states have had time to be set during changing the pulse parameters. Bearing in mind that for fast vibronic relaxation

$$\Delta'(\alpha, t) = \frac{n_1(t)}{(2\pi\sigma_{2s})^{1/2}} \exp\left(-\frac{\alpha^2}{2\sigma_{2s}^2}\right) - \frac{n_2(t)}{(2\pi\sigma_{2s})^{1/2}} \exp\left[-\frac{(\alpha - \omega_{st})^2}{2\sigma_{2s}^2}\right], \quad (29)$$

substituting the last equation into Eq.(28), one gets Eq.(6) of the main text. The latter contains the line-shape functions

of a monomer molecule for the absorption (fluorescence) for fast vibronic relaxation, $-\dot{i}W_{a(f)}(\omega)$. For the "slow modulation" limit considered in the beginning of Section 2, these quantities are given by [15]

$$W_{a(f)}(\omega) = \sqrt{\frac{1}{2\pi\sigma_{2s}^2}} w\left(\frac{\omega - \omega_{21} + \delta_{a(f),f}\omega_{st}}{\sqrt{2\sigma_{2s}^2}}\right) \quad (30)$$

where $w(z) = \exp(-z^2)[1 + i\operatorname{erfi}(z)]$ is the probability integral of a complex argument [25], and the absorption (fluorescence) lineshapes $\operatorname{Re}W_{a(f)}(\omega) \equiv F_{a(f)}(\omega)$ are given by

$$F_{a(f)}(\omega) = \sqrt{\frac{1}{2\pi\sigma_{2s}^2}} \exp\left[-\frac{(\omega_{21} - \omega - \delta_{a(f),f}\omega_{st})^2}{2\sigma_{2s}^2}\right] \quad (31)$$

In the case of the Gaussian modulation of the electronic transition by the vibrations the absorption lineshape is given by [28, 9, 8]

$$F_a(\omega) = \frac{1}{\pi} \operatorname{Re} \int_0^\infty \exp[i(\omega - \omega_{21})t + g(t)]dt \quad (32)$$

where

$$g(t) = - \int_0^t dt' (t - t') K(t') \quad (33)$$

is the logarithm of the characteristic function of the spectrum of single-photon absorption after subtraction of a term which is linear with respect to t and determines the first moment of the spectrum, $K(t)$ is the correlation function. Eq.(32) can be used in general case when the "slow modulation" limit is not realized. Then the monomer spectrum is given by

$$W_a(\omega) = \frac{1}{\pi} \int_0^\infty \exp[i(\omega - \omega_{21})t + g(t)]dt \quad (34)$$

For the exponential correlation function $K_s(t) = \sigma_{2s} \exp(-|t|/\tau_s)$, we get

$$g_s(t) = -\sigma_{2s}\tau_s^2 [\exp(-t/\tau_s) + \frac{t}{\tau_s} - 1] \quad (35)$$

that leads to Eq.(36) of Appendix 2.

7. Appendix 2. Description of the absorption of J-aggregates

Applying expression $\operatorname{Re}\{\bar{W}_a(\omega)/[1 - ip\pi W_a(\omega)]\}$ on the right-hand-side of Eq.(11) to the description of the absorption of J-aggregates, one should take into account that the Gaussian shape of the monomer absorption spectrum obtained in the "slow modulation" limit, Eq.(31), is correct only near the absorption maximum. The wings decline much slower as $(\omega_{21} - \omega)^{-4}$ [29]. At the same time, the expression under discussion has a pole, giving strong absorption, when $1/(p\pi) = -\operatorname{Im}W_a(\omega)$. If parameter of the dipole-dipole intermolecular interaction p is rather large, the pole may be at a large distance from the absorption band maximum where the "slow modulation" limit breaks

down. This means one should use exact expression for the monomer spectrum W_a that is not limited by the "slow modulation" approximation, and properly describes both the central spectrum region and its wings. The exact calculation of the vibrationally equilibrium monomer spectrum for the Gaussian-Markovian modulation with the exponential correlation function $S(t) = \exp(-|t|/\tau_s)$ gives [29, 28] (see Eqs.(34) and (35))

$$W_a(\omega) = \frac{\tau_s}{\pi} \frac{\Phi(1, 1 + x_a; \sigma_{2s}\tau_s^2)}{x_a} \quad (36)$$

where $x_a = \tau_s/(2T_1) + \sigma_{2s}\tau_s^2 + i\tau_s(\omega_{21} - \omega)$, $\Phi(1, 1 + x_a; \sigma_{2s}\tau_s^2)$ is a confluent hypergeometric function [25]. Eq.(36) is used for calculating the nonlinear absorption spectra of J-aggregates in Section 2.1.1.

8. Appendix 3. Description of the absorption of H-aggregates

To describe the absorption of H-aggregates, one should take also HFOA intramolecular vibrations into account, in addition to the LFOA vibrations $\{\omega_s\}$. The extension of Eq.(11) to the presence of the HFOA vibrations carried out in Section 3, enables us to use previous expression $\operatorname{Re}\{W_a(\omega)/[1 - ip\pi W_a(\omega)]\}$ (see Section 2.1.1) for the description of the absorption of H-aggregates where the monomer spectrum W_a should include the contribution from the HFOA intramolecular vibrations. We will consider one normal high frequency intramolecular oscillator of frequency ω_0 whose equilibrium position is shifted under electronic transition. Its characteristic function $f_{\alpha M}(t)$ is determined by the following expression [4]:

$$f_{\alpha M}(t) = \exp(-S_0 \coth \theta_0) \sum_{k=-\infty}^{\infty} I_k(S_0 / \sinh \theta_0) \times \exp[k(\theta_0 + i\omega_0 t)] \quad (37)$$

where S_0 is the dimensionless parameter of the shift, $\theta_0 = \hbar\omega_0/(2k_B T)$, $I_n(x)$ is the modified Bessel function of first kind [25]. Then $W_a(\omega)$ can be written as

$$\begin{aligned} W_a(\omega) &= \frac{1}{\pi} \int_0^\infty f_{\alpha M}^*(t) \exp[i(\omega - \omega_{21})t + g_s(t)]dt \\ &= \sum_{k=-\infty}^{\infty} \frac{\exp(-S_0 \coth \theta_0 + k\theta_0)}{\pi} I_k\left(\frac{S_0}{\sinh \theta_0}\right) \\ &\quad \times \int_0^\infty \exp[i(\omega - k\omega_0 - \omega_{21})t + g_s(t)]dt \end{aligned}$$

where $g_s(t)$ is given by Eq.(35) of Appendix 1. Integrating with respect to t , one gets Eq.(13) of the main text for $\theta_0 \gg 1$.

References

- [1] K. Takazawa, J. Inoue, K. Mitsuishi, and T. Takamasu, "Fraction of a millimeter propagation of exciton polaritons in photoexcited nanofibers of organic dye," *Phys. Rev. Letters*, vol. 105, p. 067401, 2010.

[2] K. Takazawa, J. Inoue, K. Mitsuishi, and T. Kuroda, “Ultracompact asymmetric mach-zehnder interferometers with high visibility constructed from exciton polariton waveguides of organic dye nanofibers,” *Advanced Functional Materials*, vol. 23, no. 7, pp. 839–845, 2013.

[3] B. D. Fainberg, “Nonperturbative analytic approach to interaction of intense ultrashort chirped pulses with molecules in solution: Picture of “moving” potentials,” *J. Chem. Phys.*, vol. 109, no. 11, pp. 4523–4532, 1998.

[4] B. D. Fainberg and V. Narbaev, “Chirped pulse excitation in condensed phase involving intramolecular modes studied by double-sided Feynman diagrams for fast electronic dephasing,” *J. Chem. Phys.*, vol. 113, no. 18, pp. 8113–8124, 2000.

[5] ———, “Chirped pulse excitation in condensed phase involving intramolecular modes. ii. absorption spectrum,” *J. Chem. Phys.*, vol. 116, no. 11, pp. 4530–4541, 2002.

[6] M. V. Klein and T. E. Furtak, *Optics*. New York: Wiley, 1988.

[7] A. Eisfeld and J. S. Briggs, “The j- and h-bands of organic dye aggregates,” *Chem. Phys.*, vol. 324, pp. 376–384, 2006.

[8] B. D. Fainberg, in *Advances in Multiphoton Processes and Spectroscopy*, S. H. Lin, A. A. Villaey, and Y. Fujimura, Eds. Singapore, New Jersey, London: World Scientific, 2003, vol. 15, pp. 215–374.

[9] S. Mukamel, *Principles of Nonlinear Optical Spectroscopy*. New York: Oxford University Press, 1995.

[10] B. D. Fainberg, *Opt. Spectrosc.*, vol. 68, p. 305, 1990, [Opt. Spektrosk., vol. 68, 525, 1990].

[11] B. Fainberg, *Phys. Rev. A*, vol. 48, p. 849, 1993.

[12] B. D. Fainberg, “Non-linear polarization and spectroscopy of vibronic transitions in the field of intensive ultrashort pulses,” *Chem. Phys.*, vol. 148, pp. 33–45, 1990.

[13] A. S. Davydov, *Theory of Molecular Excitons*. New York: Plenum, 1971.

[14] B. D. Fainberg and B. Levinsky, “Stimulated raman adiabatic passage in a dense medium,” *Adv. Phys. Chem.*, vol. 2010, p. 798419, 2010.

[15] B. D. Fainberg and G. Li, “Nonlinear organic plasmonics: Applications to optical control of coulomb blocking in nanojunctions,” *Applied Phys. Lett.*, vol. 107, no. 5, p. 053302, 2015, [Erratum, v. 107, 109902 (2015)].

[16] H. Haug and S. W. Koch, *Quantum theory of the optical and electronic properties of semiconductors*. Singapore: World Scientific, 2001.

[17] K. Minoshima, M. Taiji, K. Misawa, and T. Kobayashi, “Femtosecond nonlinear optical dynamics of excitons in j-aggregates,” *Chem. Phys. Lett.*, vol. 218, pp. 67–72, 1994.

[18] Y. Toyozawa, “On the dynamical behavior of an exciton,” *Progr. Theor. Phys. Suppl.*, vol. 12, pp. 111–140, 1958.

[19] K. Takazawa, Y. Kitahama, Y. Kimura, and G. Kido, “Optical waveguide self-assembled from organic dye molecules in solution,” *Nano Letters*, vol. 5, no. 7, pp. 1293–1296, 2005.

[20] K. Takazawa, “Waveguiding properties of fiber-shaped aggregates self-assembled from thiacyanine dye molecules,” *J. Phys. Chem. C*, vol. 111, pp. 8671–8676, 2007.

[21] A. Eisfeld and J. S. Briggs, “The j-band of organic dyes: lineshape and coherence length,” *Chem. Phys.*, vol. 281, pp. 61–70, 2002.

[22] ———, “Absorption spectra of quantum aggregates interacting via long-range forces,” *Phys. Rev. Lett.*, vol. 96, p. 113003, 2006.

[23] V. A. Malyshev and P. Moreno, “Mirrorless optical bistability of linear molecular aggregates,” *Phys. Rev. A*, vol. 53, no. 1, pp. 416–423, 1996.

[24] B. D. Fainberg and D. Huppert, *Adv. Chem. Phys.*, vol. 107 (Chapter 3), pp. 191–261, 1999.

[25] M. Abramowitz and I. Stegun, *Handbook on Mathematical Functions*. New York: Dover, 1964.

[26] M. Litinskaya, P. Reineker, and V. M. Agranovich, “Exciton polaritons in organic microcavities,” *Journal of Luminescence*, vol. 119–120, pp. 277–282, 2006.

[27] N. J. Halas, S. Lal, W.-S. Chang, S. Link, and P. Nordlander, “Plasmons in strongly coupled metallic nanostructures,” *Chem. Rev.*, vol. 111, pp. 3913–3961, 2011.

[28] B. D. Fainberg, *Opt. Spectrosc.*, vol. 58, p. 323, 1985, [Opt. Spektrosk. v. 58, 533 (1985)].

[29] S. G. Rautian and I. I. Sobel'man, “The effect of collisions on the doppler broadening of spectral lines,” *SOVIET PHYSICS USPEKHI*, vol. 9, no. 5, pp. 701–716, 1967, [Usp. Fiz. Nauk 90, 209–238 (1966)].